Physio-Mechanical Assessment and Process Mapping of AlSi10mg/Cu Material for Automobile Application

O. Olaniran[1*], A. A. Adediran[2] A.A. Akinwande[1], O.S. Adesina[3], O.A. Mosadomi[2]
[1]Department of Metallurgical and Materials Engineering, Federal University of Technology, Akure, Ondo State, Nigeria
[2]Materials Design and Structural Integrity Research Group, Department of Mechanical Engineering, Landmark University, Omu-Aran, Kwara State, Nigeria
[3]Department of Mechatronics Engineering, Bowen University, Iwo, Osun State, Nigeria

ABSTRACT: In this study, copper (Cu) particles were used as a replacement for ceramic particles in an AlSi10Mg matrix to lessen the brittleness often associated with ceramic particles when used as fillers in aluminum matrix. AlSi10Mg was combined with 0, 2, 4, and 6% Cu, and microwave sintering was performed at 300, 450, and 600 °C. The composites produced were subjected to physical tests (porosity, density, shrinkage, and relative density), tensile tests (yield and ultimate strength, elastic modulus, and elongation), and microstructure test. Cu particles were observed to be dispersed at 2% and 4% sintering temperatures and clustered at 6% sintering temperatures, according to the microstructural images. The incorporation of 2% and 4% Cu decreased porosity, leading to increased yield, ultimate tensile strength, and elastic modulus respectively. It was noted that 6% Cu addition resulted in strength reduction owing to particle clusters. Sintering temperatures between 300 and 450 °C were favorable for all property investigated; nevertheless, temperatures above 600 °C were detrimental to property responses. The proposed process map revealed diverse response values for varying input combination parameters; hence, a Cu dosage of 4% at a sintering temperature of ≤ 450 °C is recommended.

KEYWORDS: AlSi10Mg; Lightweight; Microstructure; Microwave sintering, Process maps.

[Received Dec. 10, 2022; Revised Feb. 6, 2023; Accepted April 14, 2023] Print ISSN: 0189-9546 | Online ISSN: 2437-2110

I. INTRODUCTION

The trend in present-day engineering design involves lightweight applications. To this end, light-weight materials are sought after for engineering applications. Also, high strength, corrosion, chemical, and wear resistance are other functional requirements for this lightweight application. Designs involving aerospace, automobiles, and high-speed trains have involved these kinds of properties. One of the most sought-after materials is aluminium and its alloys. When compared with steel, aluminium is lighter but possesses lower strength. In a bid to upgrade the strength performance of aluminium alloys, various fabrication procedures have been achieved, one of which is particulate reinforcement in the development of aluminium matrix composites (AMC) (Mohanavel *et al*.,, 2018; Ikubanni *et al*.,, 2020; Adesina *et al*.,, 2022; Ogunsanya *et al*., 2022). Aluminium-AlSi10Mg is an aluminium alloy that has gained attention in automobiles and research studies have been done to improve the performance, especially for high temperature performance (Pezzato *et al*., 2020). Commonly used particulates in aluminium matrices are of synthetic ceramic origins, including MoS, TiO2, B4C, TiN, Al2O3, SiC, SiO2, ZrO2 etc. (Adediran *et al*., 2021; Balogun *et al*., 2022; Lokesh *et al*., 2022). As a result, their incorporation into the aluminium matrix has resulted in improved wear resistance and relatively high thermal stability. Equally, these reinforcing fillers have also led to improved strength performance in the composites (Verma *et al*., 2017; Adediran *et al*., 2021).

The use of ceramic particulates in improving the performance quality of an aluminium matrix entails some drawbacks. Ceramic particulates are majorly inherently brittle. Hence, despite the improvement of the base alloy, at some points, the brittle nature takes prominence, leading to loss of strength (Gupta and Srivastava 2018). Moreso, as a result of the stiffness, plastic deformation processes like cold and hot rolling, equal channel angular pressing, extrusion, etc. are limited in the composite based on lower plasticity. The effect of ductile particles like Cu on the mechanical performance of aluminium alloy is worth investigating. Atabic *et al*., (2020); and Akinribide *et al*., (2022) investigated the effect of copper on the performance of aluminium alloys employing a liquid metallurgy approach. The findings revealed improvement in the mechanical behavior of the composites with increasing Cu addition. The investigations were on the liquid metallurgy approach. In the meantime, the approach of powder metallurgy is considered in the present study. Powder metallurgy provides much greater control over porosity and consistency, with the potential for finer microstructures yielding better performance, lower material wastage, and high near-net shape tendency.

*Corresponding author: ooladayo@futa.edu.ng
doi: http://dx.doi.org/10.4314/njtd.v18i4.1492

Furthermore, many studies in metallurgy lack process maps depicting how the experimental variables yield various responses. This study was therefore conceieved to develop an AA-7075/Cu composite by powder metallurgy adopting microwave sintering at varying sintering temperatures of 300, 450, and 600 °C. Furthermore, our study intends to develop a process map for property responses at varying sintering temperatures and Cu dosages (0, 2, 4, and 6 %). By these maps, future design responses can be forecast with the input ranges, thereby lowering future experimental costs.

II. MATERIALS AND EXPERIMENTAL PROCEDURE

As received, AlSi10Mg powder (average particle size of 20 microns and purity of 99.8 %) was mixed with Cu powder (average particle size of 6 microns and purity of 99.93 %) at copper weight fractions of 0, 2, 4, and 6 %. The elemental composition of the as-received powders and the properties of the AlSi10Mg powder are presented in Tables 1 and 2 respectively. The composite powders were mixed in a tubular mix for 24 hours for homogeneity and consolidated (diameter 50 mm and length 120 mm) using a hydraulic press at a uniaxial compaction pressure of 60 MPa to obtain green samples. Sintering was done in a vacuum microwave furnace at varying temperatures of 300, 450, and 600 °C. Meanwhile, the heating rate was kept at 20°C/min until the temperatures were reached and a 25-minute dwell time was allowed. Afterwards, the samples were cooled to room temperature in the air. Cooled samples were cut into smaller sizes, then grounded and polished for microstructural evaluation. Phase characterization and diffraction patterns were measured by an X-ray diffractometer (Siemens D5000) when maintaining parameters at 40 mA and 45 KV between angles of 0 and 90 °. The density was measured by the Archimedes method while shrinkage was probed by initial measurement of green dimensions and sintered dimensions.

The percentage difference was realized as sintered shrinkage. For the examination of the mechanical properties, the samples were machined into shapes and subjected to a tensile test using a universal testing machine (INSTRON 3369) at a strain rate of 10^{-3}/s and a cross head speed of 3 mm/min, applying a load of 10 kN.

Table 1: Chemical constituents of as-received AlSi10Mg and Cu powders

	Si	Mg	Cu	Ni	Mn	Ti	Fe	Al
AlSi10Mg	10.1	0.7	0.26	0.04	0.12	0.13	0.3	Balance
Cu	-	-	99.93	-	-	-	0.04	0.3

Table 2: Properties of as-received AlSi10Mg

Density (g/cm^3)	YS (MPa)	UTS (MPa)	HD (HV)	El (%)	EM (GPa)
2.66	265.3	338.9	113	9 %	72.1

YS is yield strength, UTS is ultimate tensile strength, HD is micro hardness, El is elongation and EM is elastic modulus.

III. RESULTS AND DISCUSSIONS

A. Analysis of the diffraction pattern and microstructural features

Figures 1(a), (b), (c), (d) and Figures 2(a), (b), (c), (d) display the diffraction patterns of samples sintered at 300 and 450 °C, respectively. The images showed peaks of α-aluminium indicated as 1. In Figures 1a and 2a, the α-aluminium coexisted with the Si peaks, indicating a base alloy of AlSi10Mg. Similar peaks of aluminium and silica have been reported in Gu *et al.,* (2019); Liu *et al.,* (2019). A magnesium peak was not identified because of the low content of magnesium. At 2 % Cu addition, Cu peaks were indicated in Figures 1b and 2b. With increasing Cu dosage, the peak height increased at 4% (Figures 1c and 2c) and 6 % (Figures 1d and 2d) addition based on the increasing content of the reinforcing phase. At such sintering temperatures, the base alloy phases and reinforcing phase were well identified.

Figure 3 depicts the diffraction pattern for 600 °C composite mixes. In Figure 3a, the aluminium and silica phases were majorly present. In addition to these phases, peaks of secondary phases of Mg_2Si and $CuAl_2$ were also identified, which are possibly formed at high temperature sintering on account of liquid phase sintering since the sintering temperature of 600 °C is higher than the melting point of the base alloy (572 ± 5 °C).

The microstructure of the developed composites at varying temperatures is highlighted in Figure 4. Figures 4 a-d reveal images of sintered composites sintered at 300 °C, 4 e-h sintered at 450 °C, and 4 i - l sintered at 600 °C. Figures 4a, 4e, and 4f all showed a high level of porosity in the base alloy sintered at 300 °C, 450 °C, and 600 °C, respectively. At 2 % (Figure 4 b, f, and j) and 4 % (Figure 4 c, g, and k), the Cu particles are dispersed within the microstructure and lower porosity was observed. The Cu particles are identified by the white arrow in Figure 4. The EDX analysis carried out on the white particles dispersed showed they are Cu particles as indicated in Figure 5a. In the case of 6 % Cu addition, particle clusters (indicated by yellow arrows) were observed owing to high particle density (Akinwande *et al.,* 2022). Lower porosities are also observed relative to the base alloy (Figure 4d). The intermetallic phases identified in Figure 3 labelled m_1 ($MgSi_2$) and m_2 ($CuAl_2$) are noted to be present in Figure 4j, k, l. The result of the spot analysis carried out on labelled spots (m_1 and m_2) are presented in Figure 5b, and c respectively containing majorly silicon and magnesium as in the case of $MgSi_2$ (Fig. 5b). It is evident in $CuAl_2$ that the major elements are copper and aluminium, this is as displayed in Figure 5c.

B. Properties of designed composites

1) Physical properties

i. Porosity and sintering shrinkage

The porosity of the composites with respect to varying sintering temperatures is as shown in Figure 6a. It is observed that 2–4 % Cu particle addition for all temperatures considered depicted a decrease in porosity. This occurs owing to the infilling of pores by the particles, leading to lower porosity. As observed in the SEM image displayed in Figure 4, at 0 % Cu, there was porosity in the images for all temperatures considered. However, the inclusion of 2 and 6% resulted in lower porosity based on pore infilling.

Similar cases were observed when alumina and boron carbide particles were added to aluminium alloy matrixes by Mohammed *et al.,* (2013) and Sharma *et al.,* (2019). This observation is linked to the reduced partial contacts existing

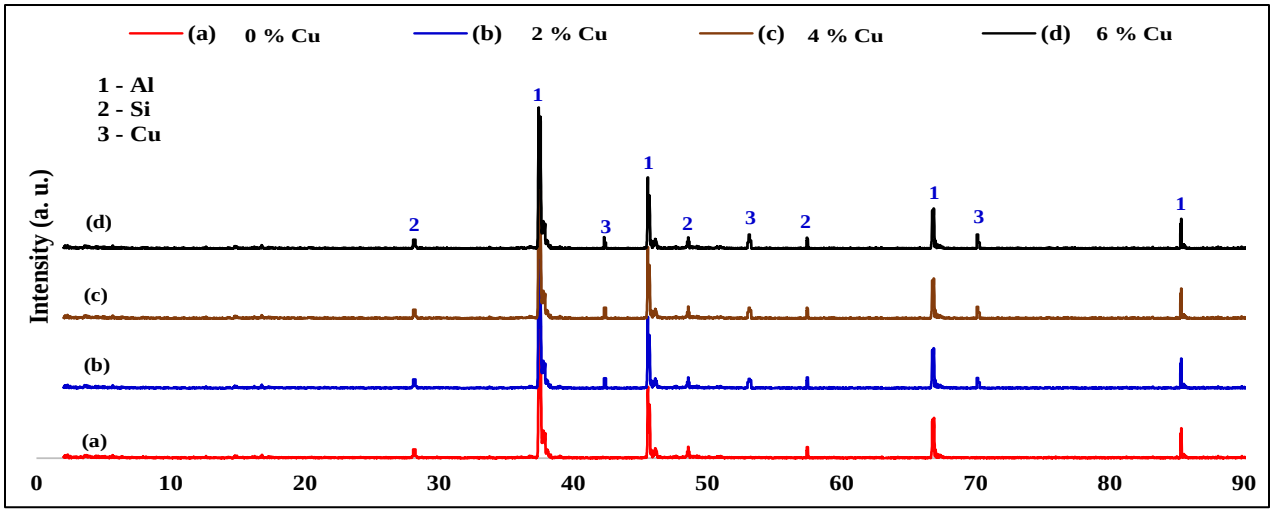

Figure 1: diffraction pattern for sintered samples at 300 ℃ for (a) 0%Cu (b) 2%Cu (c) 4%Cu and (d) 6%Cu

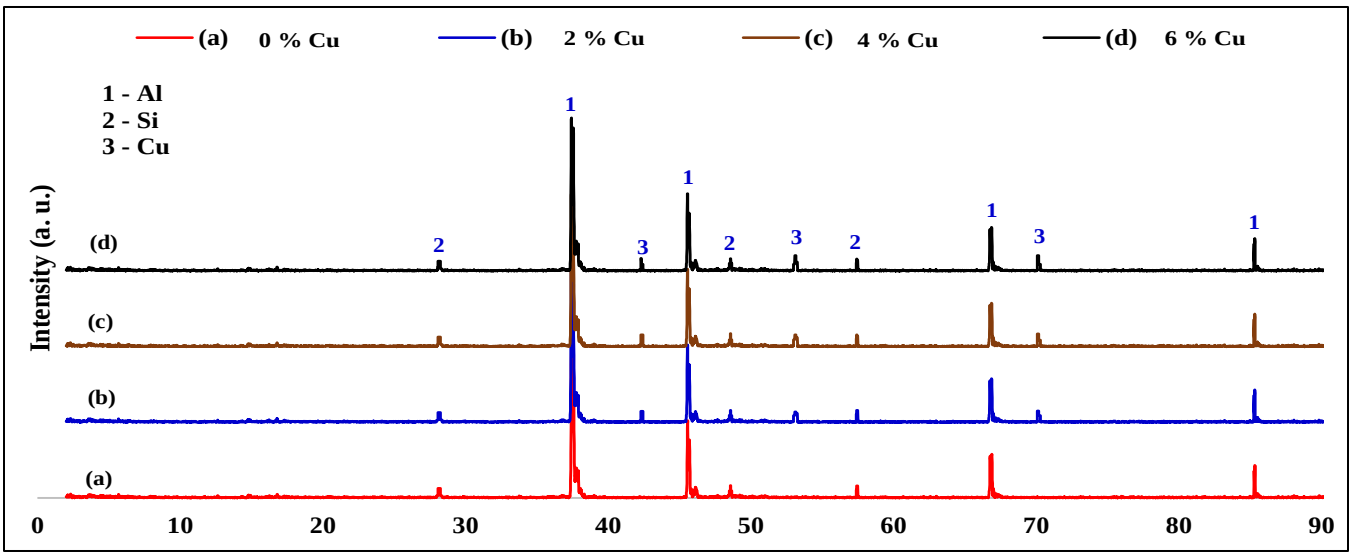

Figure 2: diffraction pattern for sintered samples at 450 ℃ for (a) 0%Cu (b) 2%Cu (c) 4%Cu and (d) 6%Cu

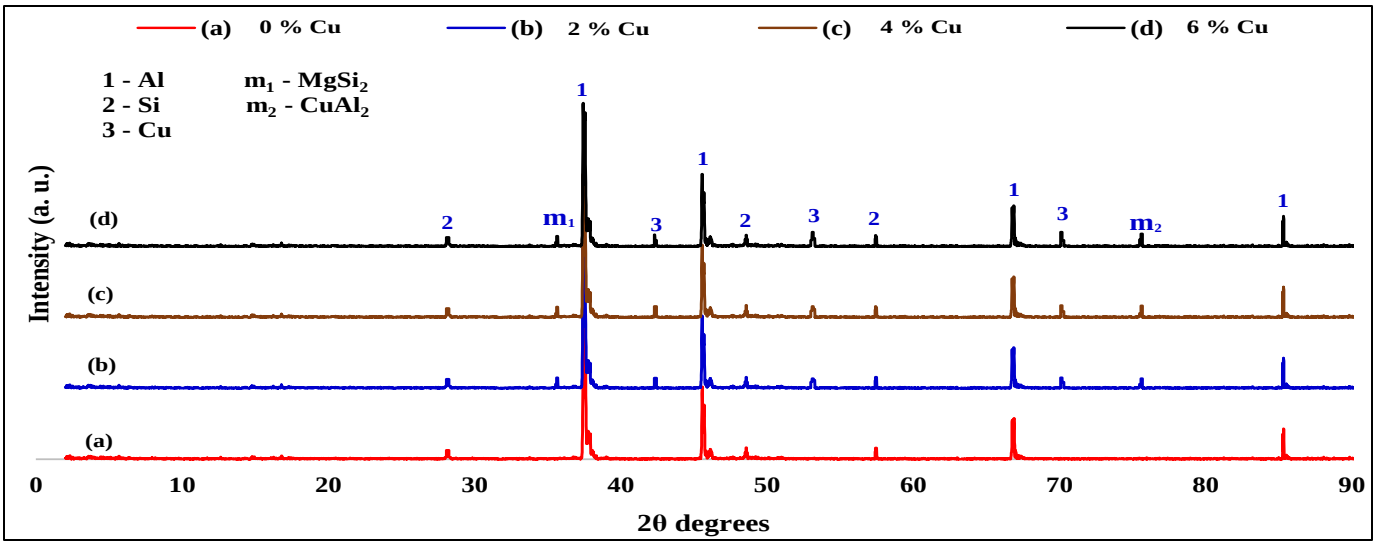

Figure 3: diffraction pattern for composites mix fabricated at 600 °C for (a) 0%Cu (b) 2%Cu (c) 4%Cu and (d) 6%Cu

among adjacent particles, resulting in increased fusion sites, leading to depreciation in interparticle voids. Tosun and Kurt (2019) and Zawrah *et al.*, (2022) both reported the same occurrence when SiC was incorporated into an aluminum matrix. The effect of sintering temperature on porosity was further presented in the plot (Figure 5).

It has also been discovered that increasing the temperature between 300 and 450 °C causes a decrease in porosity. This is associated with increased compaction and densification, leading to a decrease in interparticle distance and enhanced interparticle cohesion. Findings reported Ariff *et al.*, (2020);

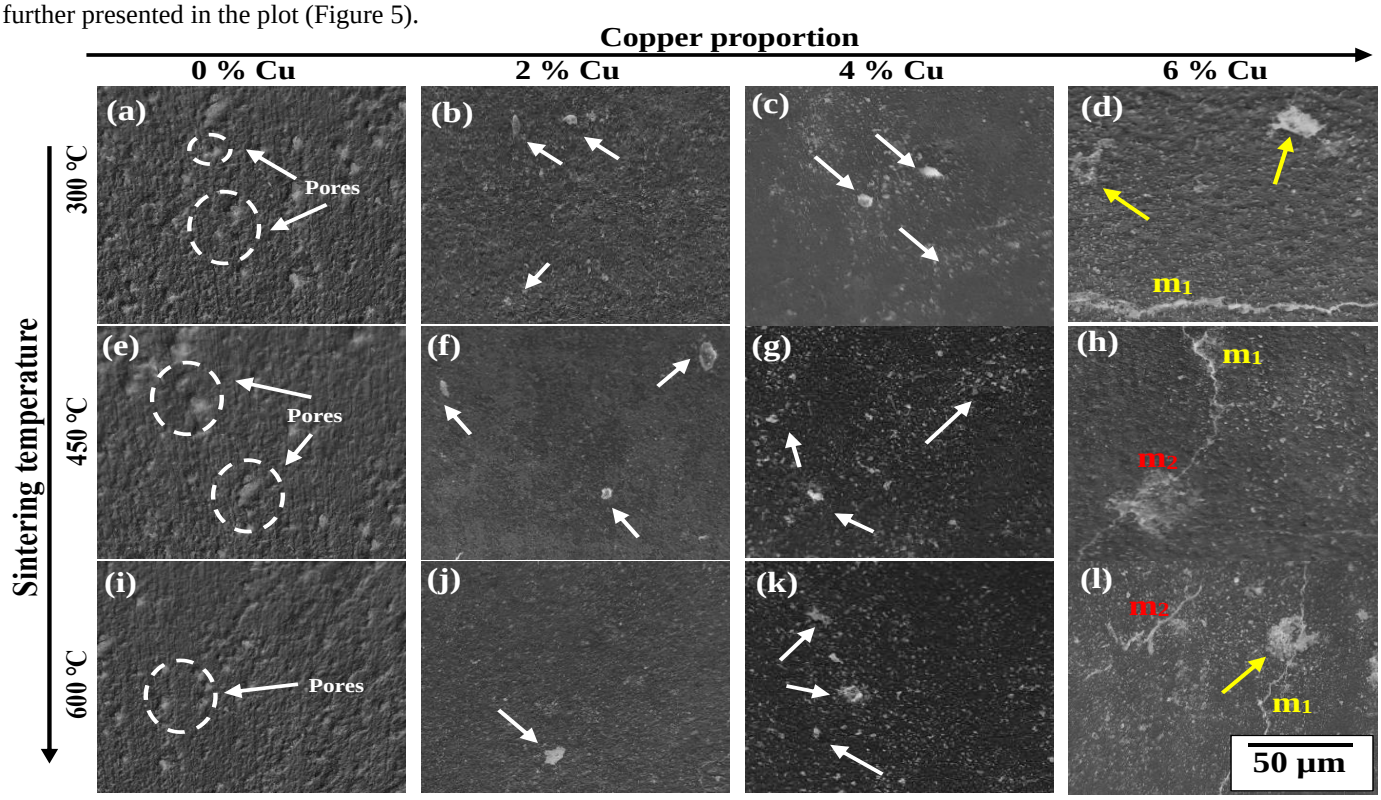

Figure 4: Microstructure of developed composites at 300 °C showing (a), (b), (c), (d); 450 °C for (e), (f), (g), (h) and for 600 °C (i), (j), (k), (l).

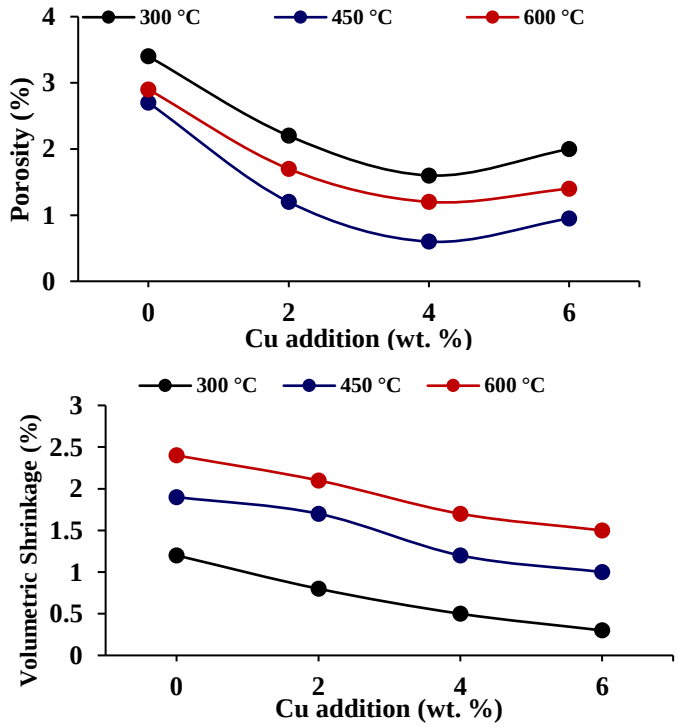

Figure 6: Relationship between Cu proportion and sintering temperature on (a) porosity and (b) volumetric shrinkage

Debnath and Pramanick (2020) revealed a decrease in porosity at increasing sintering temperatures. In this study, 0, 2, 4, and 6% Cu particles resulted in 27.8, 22.7, 14.7 and 13.1% reductions in porosity at 450 °C and 61.1, 50.0, 32.4, and 28.9% reductions at 600 °C when compared to 300 °C porosity values. While sintering at 600 °C, it was noted that porosity slightly increased for all the dosages of the Cu particles. In comparison to the porosity values obtained at 450 °C, the porosity obtained at 600 °C is greater for all corresponding doses of Cu particles. This occurred on account of the increased temperature which increased mobility of atoms and as a consequence, there is greater atomic excitation. During solidification, there is atomic rearrangement with the tendency for greater interatomic distance consequently leading to expanded voids. Moreso, during cooling, gases are evolved, ensuing a rise in porosity (Akinwande *et al.*, 2022b; Olaniran *et al.*, 2022).

Sintering shrinkage, as represented in Figure 6b, pictures that sintering shrinkage is reduced with particle addition. It is also reported that shrinkage increases with temperature owing to increased densification, compaction, and decreased interparticle distances. Arif *et al.*, (2020) demonstrated the same observation in that increasing sintering temperature resulted in an appreciation in sintering shrinkage of developed aluminium composites. They attributed the shrinkage to the decomposition of the binder used.

ii. Sintered and relative densities

Figure 7 presents the sintered density as a function of Cu particle addition and sintering temperature. As observed, the addition of the Cu particles in the aluminium matrix ensued a progressive increase in density owing to the density difference. The density of Cu is far higher than the density of the alloy (Table 2). Hence, its inclusion in the matrix at an increasing fraction is justified to result in a consecutive appreciation in sintered density. In line with our findings, Saleh *et al*., (2020) discovered an increase in density when SiCp were introduced into the aluminium-zinc matrix, demonstrating that the inclusion of higher density particles has the potential to increase the experimental density of the obtained composite. Likewise, Choudhury *et al*., (2021) recorded a consecutive increase in the density of developed aluminium composite on the inclusion of zirconia particles.

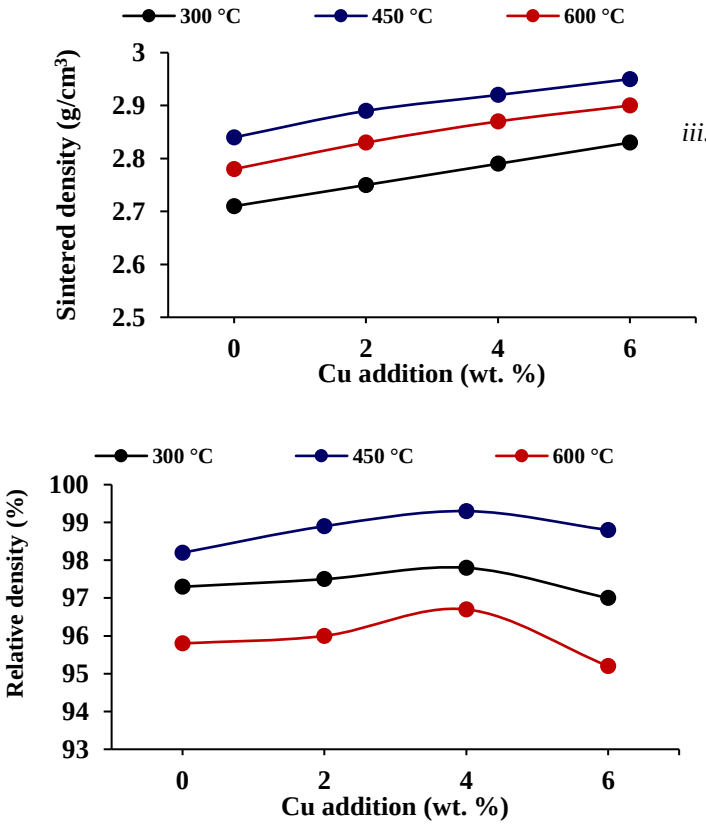

Figure 7: Relationship between Cu proportion and sintering temperature on (a) sintered density and (b) relative density.

Furthermore, increasing the sintering temperature between 300 and 450 °C amounted in a sequential increase in sintered density due to increased compartment and densification, as well as a decrease in interparticle distance owing to the closing of pores within the matrix. The implication of this observation is that between 300 and 450 °C sintering, sintering density is enhanced. Khaerudini *et al*., (2008) presented the effect of sintering temperature on the density of an aluminium-SiC composite. Temperatures between 450 and 600 °C were found to cause increased densification, which was attributed to degassing, particle interlocking, and a cohesive mechanism. Equally, Nuruzzaman *et al*., (2016) and Sun *et al*., (2018) demonstrated enhancement of the density of developed composites as sintering temperature increased. A similar observation exhibited in this study can be found in the literature by Efe *et al*., (2011) and Gurbuz *et al*., (2017). At 600 °C sintering, density is shown to decrease based on a slight increase in porosity at that temperature. Tosun and Kurt (2019) demonstrated a similar finding.

Figure 7b portrays the relative densities of the composites at varying Cu contents and sintering temperatures. In the figure, 2–6 % Cu particles resulted in appreciable relative densities on account of lower porosity. This trend, reflect an inverse relationship between porosity and relative density. Densification increased with increasing sintering temperature between 300 and 450 °C, amounting to an increase in relative density. Nevertheless, 600 °C sintering brought about a reduction in the relative density owing to increased porosity at such a temperature. A comparable study by Choudhury *et al.*, (2021) reflected how sintering temperature played a role in the relative density of the developed composite.

iii. 2) Tensile performance

The results of the yield and ultimate tensile strengths are highlighted in Figure 8 (a) and (b). For all temperatures, 2 to 4 % Cu dosage resulted in an improvement in the tensile strengths of the composites. The increase in strength is interrelated with the dispersion of the particles. The SEM image in Figure 4 highlights dispersed particles at 2 and 4 % Cu addition for all temperatures considered. As a result, dislocation motion is impeded or slowed down during tensile deformation, eventually improving tensile strength. The reports of Matli *et al*., (2020); Talabi *et al*., (2022) demonstrated the role of particle dispersion in the enhancement of tensile performance of developed aluminium composites.

For all temperatures, 6 % Cu addition displayed strength reduction, attributed to sites of particle clusters which serves as stress risers in the matrix. This observation has been reported in the literatures (Akinwande *et al*., 2022a; Ogunsanya *et al*., 2022). The SEM image in Figure 4 highlights the presence of particle clusters at a 6 % Cu addition. This is partly responsible for the strength decrease as particle clusters contribute negatively to strength (Akinwande *et al*., 2022a; Akinwande *et al*., 2022b). The tensile strengths at 600 °C were observed to be lower. The occurrence is hinged on the porosity and unfused particles in the matrix serving as points of strength weakening. In their study, Priyadarshi and Sharma (2016) portrayed the negative consequence of porosity on ductility and tensile performance of metal composites. An investigation carried out by Tatyana *et al*., (2014) revealed how sintering temperature improved the tensile performance of nickel composite between 900 and 1000 °C, of which sintering at 1100 °C resulted in strength reduction on nickel composite developed. The elastic modulus of the developed material manifested improvement as Cu particles increased, occasioned by the increased stiffness afforded by the presence of the particulate (Figure 8c). The modulus was improved between 300 and 450 °C, while 600 °C sintering spawned a lower modulus. Salinas et al., (2020) demonstrated the negative influence of porosity on elastic modulus.

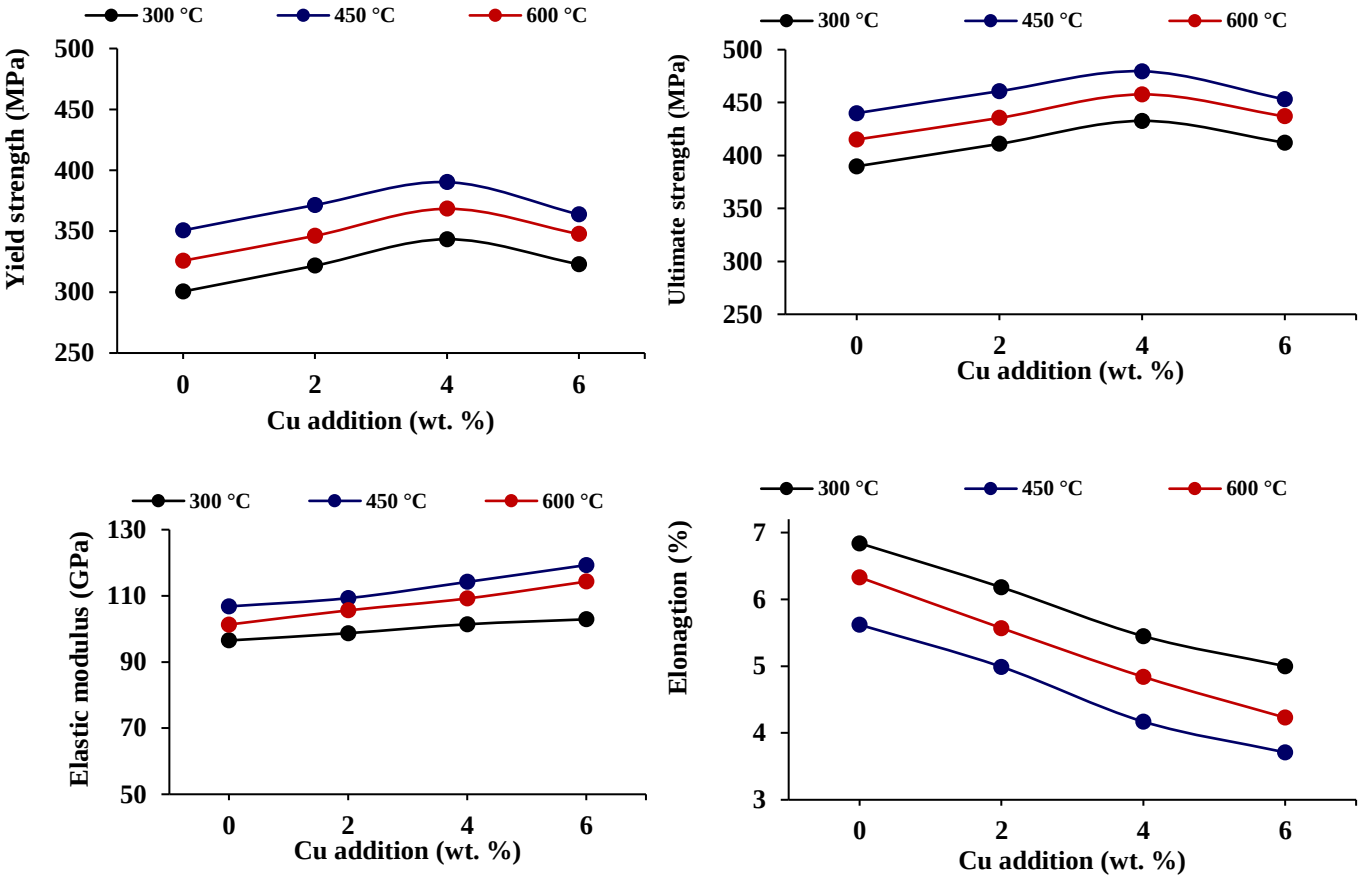

Figure 8: Relationship between Cu proportion and sintering temperature on (a) yield tensile strength and (b) ultimate tensile strength.

Similar to the findings of Razzaq *et al*., (2021), elongation was reduced with increasing particles owing to increased densification and stiffness contributed by the Cu particles (Figure 8d). Between 300 and 450 °C, for every dosage of the Cu particles, there was a reduction based on increased compaction afforded by higher sintering temperature. Somani et al., (2021) exhibited a progressive decrease in elongation with an increase in sintering temperature. Elongation was observed to slightly increase at 600 °C sintering for all weight fractions of Cu. This occurred because of the increased interatomic distance based on the increment in porosity. As a result, the obstacle to dislocation mobility was eased, permitting dislocation navigation.

The results of the yield and ultimate tensile strengths are highlighted in Figures 8 (a) and (b). For all temperatures, 2 to 6 % Cu dosage resulted in an improvement in the tensile strengths of the composites. The increase in strength is interrelated with the dispersion of the particles. The SEM image in Figure 4 highlights dispersed particles at 2 and 4 % Cu addition for all temperatures considered. As a result, dislocation motion is impeded or slowed down during tensile deformation, eventually improving tensile strength. The reports of Matli *et al.,* (2020); Talabi *et al.,* (2022) demonstrated the role of particle dispersion in the enhancement of tensile performance of developed aluminium composites.

For all temperatures, 6 % Cu addition displayed strength reduction, an occurrence hinged on the porosity and unfused particles in the matrix serving as points of strength weakening. In their study, Priyadarshi and Sharma (2016) portrayed the negative consequence of porosity on ductility and tensile performance of metal composites. This observation has been reported in the literatures (Akinwande *et al.,* 2022a; Ogunsanya *et al.,* 2022) The SEM image in Figure 4 highlights the presence of particle clusters at a 6 % Cu addition. This is partly responsible for the strength decrease as particle clusters contribute negatively to strength (Akinwande *et al.,* 2022a; Akinwande *et al.,* 2022b). The tensile strengths at 600 °C were observed to be lower on account of liquid phase sintering, which resulted in increased composite porosity. An investigation carried out by Tatyana *et al.,* (2014) revealed how sintering temperature improved the tensile performance of nickel composite between 900 °C and 1000 °C, of which sintering at 1100 °C resulted in strength reduction on nickel composite developed. The elastic modulus of the developed material manifested improvement as Cu particles increased, occasioned by the increased stiffness afforded by the presence of particulate (Figure 8c). At 300 °C, 6 % Cu addition ensued in lower modulus because of increased porosity, which lowered the stiffness based on increased inter-particle distance. The modulus was improved between 300 °C and 450 °C, while 600 °C sintering spawned a lower modulus. Salinas *et al.,* (2020) demonstrated the negative influence of porosity on elastic modulus.

Similar to the findings of Razzaq *et al.,* (2021), elongation was reduced with increasing particles owing to increased densification and stiffness contributed by the Cu

particles. Between 300 °C and 450 °C, for every dosage of the Cu particles, there was a reduction based on increased compaction afforded by higher sintering temperature. Somani *et al.*, (2021) exhibited a progressive decrease in elongation with an increase in sintering temperature. Elongation was observed to slightly increase at 600 °C sintering for all weight fractions of Cu. This occurred because of the increased interatomic distance based on the increment in porosity. As a result, the obstacle to dislocation mobility was eased, permitting dislocation navigation.

3) Process Map and Interpretation

According to Akinwande *et al*., (2021); Akinwande *et al*., (2022c), a 2-dimensional process map is a plot involving the connection of varying points by lines called contour lines. This map gives a view of how varying response values can be attained at varying combinations of inputs by which maximum or minimum response values can be obtained. A similar report can be found in literatures Olaniran et al. (2022); Akinwande *et al*. (2023a), (2023b); Daramola *et al*. (2023). Figure 9 presents the process map for the eight responses in this investigation. In the figure, two regions are identified and labelled. The blue region marked as "Min" is the region in which maximum response values are obtained, while the region marked "Max" is the region for maximization of response. The regions with mixed yellow-green-sky blue colors are the intermediate regions where average responses are obtained.

For the physical properties, porosity, shrinkage, sintered density, (Figure 9 a, b, c), minimum response values are desirable since the composite developed should be light with less porosity and shrinkage. Therefore, the blue region (Min) is desirable. In that case, for minimization of porosity, shrinkage and sintered density, input parameters should be combined in the range of 2.6 – 4.7 % Cu and 375 °C – 600 °C sintering temperature for a minimal porosity range of 2.315 – 2.24 %. In order to minimize shrinkage between 0.5625 – 0.3000 %, the input combination of 3.6 – 6 % Cu and 300 °C – 335 °C sintering temperature is desirable, while that of sintering density is 0 – 1.45 % Cu and 300 °C – 335 °C for a density range of 2.740 – 2.710 g/cm3. Higher relative density is desirable for increased densification and compaction guaranteeing improved mechanical properties.

As a result, the region labeled "Max" is preferable, ranging from 98.79 to 99.30% value realization when Cu is in the range of 1.8 – 6.0 % and sintering temperature in the range of 410 °C – 465 °C.

With regards to mechanical properties, maximum values are desirable; hence, regions marked "Max" in red in Figure 9 e–h are chosen regions. At a sintering temperature of 415 °C – 530 °C, 2.5 – 4.65 % Cu is required for the maximum yield strength in the range of 379.3 – 390.5 MPa. The ultimate tensile strength of 468.7 – 480.0 MPa can be maximized with the input variables 2.7 – 4.7 % Cu and 415 °C – 530 °C temperature. When 4.7 – 6.0% Cu is added into the matrix at a sintering temperature of 425 °C – 540 °C, an elastic modulus of 116.3 – 119.3 MPa is obtained. It is preferable to have an elongation range of 6.449 – 6.840% at Cu range of 0 – 1.2 %, and a sintering temperature of 300 °C – 420 °C.

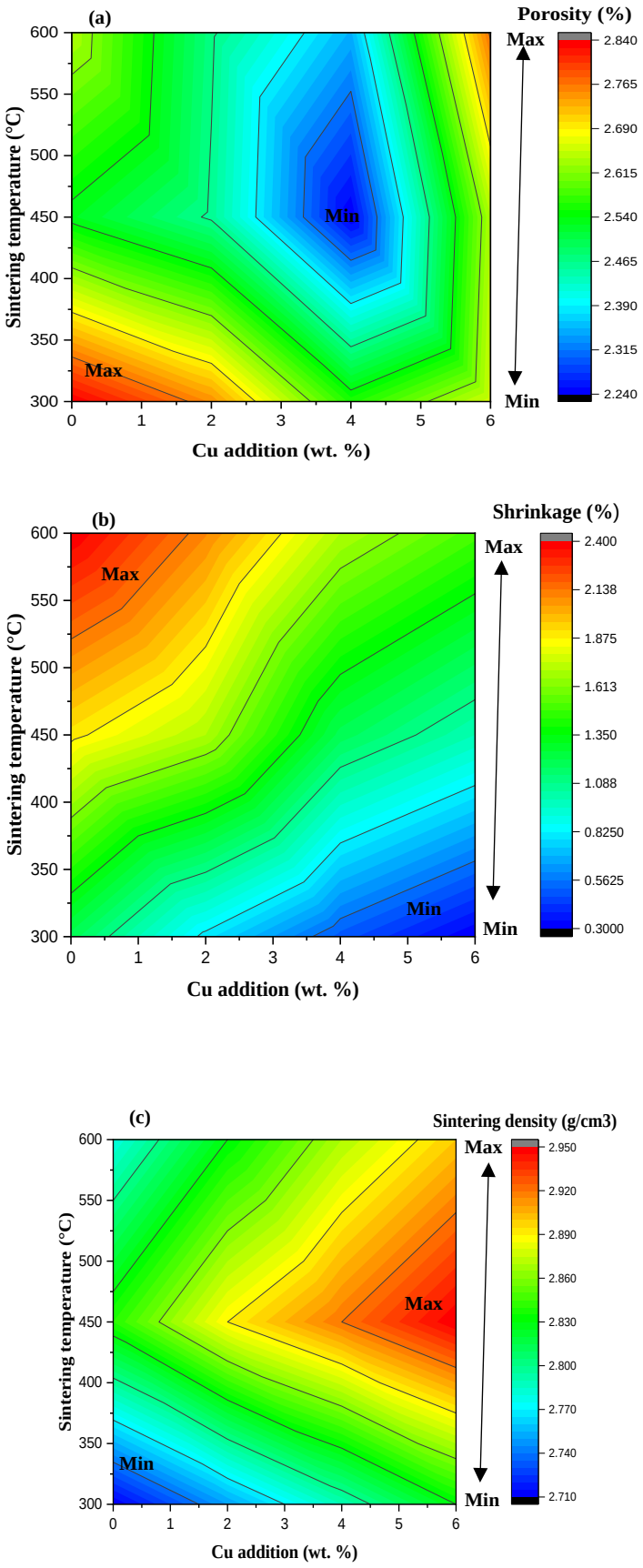

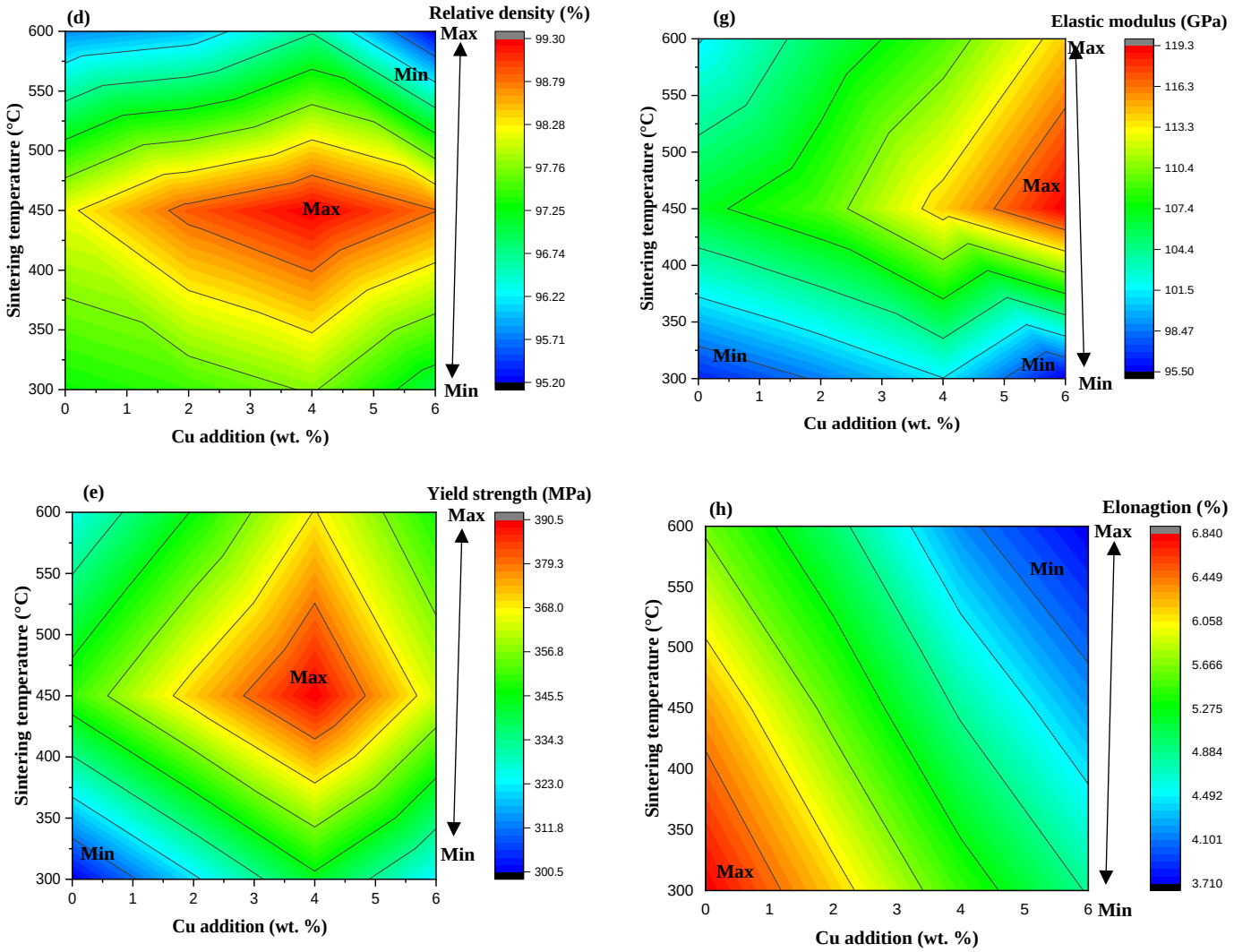

Figure 9: Process map for experimental responses (a) porosity (b) shrinkage (c) sintered density (d) relative density (e) yield strength (f) ultimate tensile strength (g) elastic modulus (h) elongation.

According to Akinwande *et al.*, (2021); Akinwande *et al.*, (2022c), a 2-dimensional process map is a plot involving the connection of varying points by lines called contour lines. This map gives a view of how varying response values can be attained at varying combinations of inputs by which maximum or minimum response values can be obtained. Figure 9 presents the process map for the eight responses in this investigation. In the figure, two regions were identified and labelled. The blue region marked as "Min" is the region in which maximum response values are obtained, while the region marked "Max" is the region for maximization of response. The regions with mixed yellow-green-sky blue colors are the intermediate regions where average responses are obtained.

For the physical properties, porosity, shrinkage, sintered density, (Fig. 9a, b, c), minimum response values are desirable since the composite developed should be light with less porosity and shrinkage. Therefore, the blue region (Min) is desirable. In that case, for minimization of porosity, shrinkage and sintered density, input parameters should be combined in the range of 2.6 – 4.7 % Cu and 375 ℃– 600 ℃ sintering temperature for a minimal porosity range of 2.315 – 2.24 %. In

order to minimize shrinkage between 0.5625 – 0.3000 %, the input combination of 3.6 – 6 % Cu and 300 ℃ – 335 ℃ sintering temperature is desirable, while that of sintering density is 0 – 1.45 % Cu and 300 ℃ – 335 ℃ for a density range of 2.740 – 2.710 g/cm^3. Higher relative density is desirable for increased densification and compaction ensuring improved mechanical properties. As a result, the region labeled "Max" is preferable, ranging from 98.79 to 99.30% value. With Cu in the range of 1.8 – 6.0 % and sintering temperature in the range of 410 ℃– 465 ℃.

It is noted in the mechanical properties that maximum values are desirable; hence, regions marked "Max" in red in Figure 9 e–h are the chosen regions. At a sintering temperature of 415 ℃ – 530 ℃, 2.5 – 4.65 % Cu is required for the maximum yield strength in the range of 379.3 – 390.5 MPa. The ultimate tensile strength of 468.7 – 480.0 MPa can be maximized in the input variables 2.7– 4.7 % Cu and 415 ℃ – 530 ℃ temperature. When 4.7 – 6.0% Cu is added into the matrix at a sintering temperature of 425 ℃ – 540 ℃, an elastic modulus of 116.3 – 119.3 MPa is obtained. It is preferable to have an elongation range of 6.449 – 6.840% at Cu range of 0 – 1.2 %, and a sintering temperature of 300 ℃ – 420 ℃.

IV. CONCLUSION

Composites were fabricated by combining Cu at 0, 2, 4, and 6% with aluminum powder and sintering at 300 ℃, 450 ℃, and 600 ℃. It was observed that pores were present at 0% Cu for all temperatures considered. The addition of 2 to 6 % Cu led to a reduction in porosity as the particles were dispersed in the matrix. It was observed that a progressive rise in Cu from 2 to 6 % spawned a progressive reduction in sintering shrinkage and elongation with a linear rise in density. Meanwhile, the study revealed that at 6 %Cu, there was existence of clusters as observed in the microstructure. Yield and ultimate tensile strengths were improved between 2 and 4 % Cu addition, while 6 % Cu resulted in strength reduction on account of particle clusters. 300 ℃ to 450 ℃ sintering temperature was favorable to densification and property improvement, while 600 ℃ sintering temperature was detrimental to the measured properties. Process maps developed revealed diverse response values at varying input combinations. From the results, it is concluded that Cu particles with 4 % maximum are desirable at a sintering temperature of not greater than 450 ℃.

AUTHOR CONTRIBUTIONS

O. Olaniran, A. A. Adediran, A.A. Akinwande: Conceptualization, Software, Validation, Writing – original draft. **O. Olaniran, A. A. Adediran:** Conceptualization, Methodology, Supervision. **O.S. Adesina, O.A. Mosadomi:** Writing – review & editing.

REFERENCES

Abdulsahib, Y. M. (2014). Effect of copper addition on the microstructure and mechanical properties of Al-Si alloy. Al-Qadisiya Journal of Engineering Sciences. 7(4), 366 – 382.

Adediran, A. A.; A. A. Akinwande; O. A. Balogun; B. J. Olorunfemi and M. S. Kumar. (2021a). Optimization studies of stir casting parameters and mechanical properties of TiO_2 reinforced Al 7075 composite using response surface methodology. Scientific Reports. 11(1), 19860. https://doi.org/10.1038/s41598-021-99168-1.

Adediran, A. A.; A. A. Akinwande; O. A. Balogun; O. S. Adesina; A. Olayanju and T. Mojisola. (2021b). Evaluation of the properties of Al-6061 alloy reinforced with particulate waste glass. Scientific African. 12, e00812. https://doi.org/j.sciaf.2021.e00812.

Adediran, A. A.; A. A. Akinwand;, O. A. Balogun; O. S. Adesina; A. Olayanju and T. Mojisola. (2021c). Evaluation of the properties of Al-6061 alloy reinforced with particulate waste glass. Scientific African. 12, e00812. https://doi.org/j.sciaf.2021.e00812

Adeosun, S. O.; S. A. Balogun; L. O. Osoba; W. A. Ayoola and A. M. Oladoye. (2011). Effect of Cu and Zn addition on the mechanical properties of structural aluminium alloy. Journal of Modern Manufacturing Technology. 3(1), 103 – 110.

Adesina, O. S.; A. A. Adediran; A. A. Akinwande; O. O. Daramola and O. Sanyaolu. (2022). Modelling and optimizing tensile behavior of developed aluminium hybrid composite. Surface review and letters. https://doi.org/10.1142/S0218625X22501207.

Akinribide, O. J.; O. O. Ogundare; S. O. Akinwamide; F. Gamaoun and P. A. Olubambi. (2022). Alloying effect of copper in AA-7075 aluminium composite using bale out furnace. Journal of Materials Research and Technology. 18, 3849 – 3856. https://doi.org/10.1016/j.jmrt.2022.04.054.

Akinwande, A. A.; A. A. Adediran; O. A. Balogun; B. J. Olorunfemi; M. S. Kumar. (2021). Optimization of flexural strength of recycled polyethylene-terephthalate (PET) eco-composite using response surface methodology. E3S Web of Conferences. 309(12), 01094. https://10.1051/e3sconf/202130901094

Akinwande, A. A.; A. A. Adediran; O. A. Balogun; M. Yibowei; A. Barnabas; H. K. Talabi; B. J. Olorunfemi. (2022b). Optimization of selected casting parameters on the mechanical behavior of Al 6061/glass powder composites. https://doi.org/10.1016/j.heliyon.2022.e09350.

Akinwande, A. A.; O. S. Adesina; A. A. Adediran; O.A. Balogun; D. Mukuro; O. P. Balogun; K. F. Tee; M. S. Kumar. (2023b). Microstructure, process optimization, and strength response modelling of green-aluminium-6061 composite as automobile material. Ceramics. 6, 386 – 415. https://doi.org/10.3390/ceramics6010023.

Akinwande, A. A.; O. A. Balogun; A. A. Adediran; O. S. Adesina; V. Romanovski ;T. C. Jen. (2023a). Experimental analysis, statistical modeling, and parametric optimization of quinary-$(CoCrFeMnNi)_{100-x}/TiC_x$ high-entropy-alloy (HEA) manufactured by laser additive manufacturing. Results in Engineering. 17, 100802. https://doi.org/10.1016/j.rineng.2022.100802.

Akinwande, A. A.; D. O. Folorunso; O. A. Balogun; H. Danso; V. Romanovski. (2022c). Paperbricks produced from wastes: modeling and optimization of compressive strength by response surface approach. Environmental Science

and Pollution Research. https://doi.org/10.1007/s11356-022-22774-7.

Akinwande, A. A.; O. A. Balogun and V. Romanovski, (2022a). Modeling, multi-response optimization, and performance reliability of green metal composites produced from municipal wastes. Environmental Science and Pollution Research. https://doi.org/10.1007/s11356-022-20023-5.

Ariff, A. H. M.; M. A. M. Najib; S. M. Tahir; A. As'Arry and M. Mazlan. (2020). Effect of sintering temperature on the properties of porous Al_2O_3-10 wt.% RHA/10 wt.% Al composite. Advances in Materials and Processing Technologies. https://doi.org/10.1080/2374068X.2020.1785204.

Atabic, D.; Z. Z. Brodarac and L. Li. (2020). Influence of copper addition in $AlSi_7MgCu$ alloy on microstructure development and tensile strength improvement. Metals. 10(1623), 1 – 16. https://doi.org/10.3390/met10121623.

Balogun, O. A.; A. A. Akinwande; O. A. Oginsanya; A. O. Ademati; A. A. Adediran; T. J. Erinle and E. T. Akinlab., (2022). Central composite design and optimization of selected stir casting parameters on flexural strength and fracture toughness $mTiO_2$/Al 7075 composites. Materials Today: Proceedings. https://doi.org/10.1016/j.matpr.2022.05.315.

Cao, C.; D. Chen; X. Fang; J. Ren; J. Shen; L. Meng; J. Liu; L. Qju and Y. Fang. (2020). Effects of Cu addition on the microstructure and properties of the Al-Mn-Fe-Si alloy. Journal of Alloys and Compounds. 834, 155175. https://doi.org/10.1016/j.jallcom.2020.155175.

Choudhury, A.; J. Nanda and S. N. Das. (2021). Sintering sensitivity of aluminium metal matrix composites developed through powder metallurgy proposed technique – a review. Journal of Physics: Conference Series. 2070, 012193. https://doi.org/10.1088/1742-6596/2070/1/012193.

Daramola, O. O.; A. A. Akinwande; A. A. Adediran; O. A. Balogun; J. L. Olajide; K. J. Adedoyin; B. O. Adewuyi and T. C. Jen. (2023). Optimization of the mechanical properties of polyester/coconut shell ash (CSA) composite for light-weight engineering applications. Scientific Reports. 13, 1066. http://doi.org/10.1038/s41598-022-26632-x.

Debnath, S. and Pramanick, A. K. (2020). Study on various properties of fabricated crystalline silica reinforced aluminium metal matrix composites. Topics in Intelligent Computing and Industry Design. 2(2), 147-150. http://doi.org/10.26480/etit.02.2020.147.150.

Efe, G. C.; T. Yener; I. Altinsoy; M. Ipek S. and Zeytin, C. Bindal. (2011). The effect of sintering temperature on some properties of Cu-SiC composite. Journal of Alloys and Compounds. 509, 6036 – 6042. https://doi.org/j.jallcom.2011.02.170

Gu, X. H.; J. X. Zhang; X. L. Fan and L. C. Zhang. (2019). Corrosion behavior of selective laser melted $AlSi_{10}Mg$ alloy in NaCl solution and its dependence of heat treatment. Acta Metallurgical Sinica. https://doi.org/10.1007/s40195-019-00903-5.

Gupta, P. K. and Srivastava, R. K.. (2018). Fabrication of ceramic reinforcement aluminium and its alloys metal matrix composite materials: A review. Materials Today: Proceedings. 5, 18761 – 18775. https://doi.org/10.1016/j.matpr.2018.06.223.

Gurbuz, M.; M. C. Senel and E. Koc. (2017). The effect of sintering time, temperature, and graphene addition on the hardness and microstructure of aluminium composites. Journal of Composite Materials. https://doi.org/10.1177/0021998317740200.

Ikubanni, P. P.; M. Oki and A. A. Adeleke. (2020). A review of ceramic/bio-based hybrid reinforced aluminium matrix composites. Cogent Engineering. 7, 1727167. https://doi.org/10.1080/23311916.2020.1727167.

Injor, O.M.; O.O. Daramola ;B.O. Adewuyi; A.A. Adediran; M.M. Ramakokovhu; R.E. Sadiku and E.T. Akinlabi. (2022). Results in Engineering, 16, 100739, https://doi.org/10.1016/j.rineng.2022.100739.

Khaerudini, D. S.; A. P. Tekudo and M. Ginting. (2008). Effect of sintering temperature and 5 wt. % $Al(NO_3)_3$ additive to metal matrix composites characteristics by powder metallurgy technique. Jutnsl Fisika Himpunan Fisika Indonesia. 8(1), 1 – 9.

Liu, B.; B. Q. Li and Z. Li. (2019). Selective laser remelting of an additive layer manufactured process on $AlSi_{10}Mg$. Results in Physics. 12, 982 – 988. https://doi.org/10.1016/j.rinp.2018.12.018.

Lokesh, N.; T. Sudheerreddy; N. G. Siddeshkumar and K. Kotresh. (2022). Characterization and evaluation of microstructure and mechanical properties of ZrO_2 reinforced Al6061 metal matrix composite using stir casting process. Advances in Materials and Processing Technologies. https://doi.org/10.1080/2374068X.2022.2066296.

Matli, P. R.; V. Manakari; G. Parande; M. R. Mattli; R. A. Shakoor and M. Gupta. (2020). Improving mechanical, thermal and damping properties of NiTi (nitinol) reinforced aluminium nanocomposite. Journal of Composite Science. 4(19), 1 – 12. https://doi.org/10.3390/jcs4010019.

Mohammed, M. M M.; O. A. Elkady and A. W. Abdelhameed. (2013). Effect of alumina particles addition on physio-mechanical properties of Al-matrix composites. Open Journal of Metals. 3, 72 – 79. https://doi.org/10.4236/ojmetal.2013.34011.

Mohanavel, V.; S. S. Kumar; T. Sathish; T. Adithiya and and K. Mariyappan. (2018). Microstructure and mechanical properties of hard ceramic particulate reinforced AA 7075 alloy composites via liquid metallurgy route. Materials Today: Proceedings. 5, 26860 – 26865. https://doi.org/10.1016/j.matpr.2018.08.168.

Nuruzzaman M.; F. F. B. Kamaruzaman and N. B. M. Azmi. (2016). Effect of sintering temperature on the properties of aluminium-aluminium oxide composite materials. International Journal of Engineering Materials and Manufacture. 1(2), 59 – 64. https://doi.org/10.26776/ijemm.01.02.2016.03.

Ogunsanya O. A.; A. A. Akinwande; O. A. Balogun; V. Romanovski and M. S. Kumar. (2022). Mechanical and damping properties of artificially aged Al 6061/TiO_2 reinforced composites for aerospace application. Particulate Science and Technology. https://doi.org/10.1080/02726351.2022.2065652.

Olaniran, O. A. A; Akinwande; A. A. Adediran and T. C. Jen. (2022). Microstructural characterization and properties of aluminium 7075/Mo prepared by microwave sintering for high-strength application. Advances in Materials and Processing Technologies. https://doi.org/10.1080/2374068X.2022.2130894.

Pezzato, L.; M. Dabala; S. Gross and K. Brunelli. (2020). Effect of microstructure and porosity of $AlSi_{10}Mg$ alloy produced by selective laser melting on the corrosion properties of plasma electrolytic oxidation coatings. Surface and Coating Technology. 404, 126477. https://doi.org/10.1016/j.surfcoat.2020.126477.

Priyadarshi, D. and Sharma, R. K. (2016). Porosity in aluminium matrix composites: cause effect and defence. Materials Science: An Indian Journal. 14(4), 119 – 129.

Razzaq, A. M.; D. L. Majid; U. M. Basheer and H. S. S Aljibori. (2021). Research summary on the processing, mechanical and tribological properties of aluminium matrix composites as effected by fly ash reinforcement. Crystals. 11(1212), 1 – 20. https://doi.org/10.3390/cryst11101212.

Saleh, B.; J. Jiang; R. Fathi; Q. Xi; L. Wang and A. Ma. (2020). Study of the microstructure and mechanical characteristics of AZ91-SiCp composites fabricated by stir casting. Achieves of Civil and Mechanical Engineering. https://doi.org/10.1007/s43452-020-00071-9.

Salinas, J. E. R.; K. M. G. Jauregui; J. A. R. Serrano; A. C. Ramirez; E. H. Hernandez; A. M. Perez and V. H. G. Perez. (2020). Simulation on the effect of porosity in the elastic modulus of SiC particle reinforced Al matrix composites. Metals. 10(391), 1 – 19. https://doi.org/10.3390/met10030391.

Sharma, D. K.; M. Sharma and G. Upadhyay. (2019). Boron carbide (B_4C) reinforced aluminium matrix composites (AMCs). International Journal of Innovative Technology and Exploring Engineering. 9(1), 2194 – 2203. https://doi.org/10.35940/ijitee.A4766.119119.

Somani, N.; Y. K. Tyagi and N. K. Gupta. (2021). An investigation on the influence of sintering temperature on microstructural, physical and mechanical properties of Cu-SiC composites. Journal of Engineering, Design and Technology. https://doi.org/10.1108/JEDT-07-2021-0374.

Sun, A.; Y. Liu; D. Wang and Z. Zhou. (2018). Sintering behavior and properties of Mo-Cu composites. Advances in Materials Science and Engineering. 2018(8703986), 1 – 7. https://doi.org/10.1155/2018/8703986.

Talabi, H.; A. M. Ojomo; O. E. Folorunso; J. F. Akinfolarin; J. P. Kumar; R. R. Mohan; A. A. Akinwande and M. S. Kumar. (2022). Development of hybrid aluminium alloy composites modified with locally sourced environmental wastes. Advances in Materials and Processing Technology. https://doi.org/10.1080/2374068X.2022.2096831.

Tatyana, S.; M. Vyacheslav; A. Alexander; K. Michail; S. Lilia and B. Sayina. (2014). Structure and properties of multilayered composite materials "Nickel-Nickel Aluminide" obtained using SPS method. Advanced Materials Research. 1040, 161 – 165. https://doi.org/10.4028/www.scientific.net/AMR.1040.161.

Tosun, G. and Kurt. M. (2019). The porosity, microstructure, and hardness of Al-Mg composites reinforced with micro particle SiC/Al_2O_3 produced using powder metallurgy. Composites Part B. 174, 106965. https://doi.org/j.compositeb.2019.106965.

Verma, N.; P. S. Rao and S. C. Vettivel. (2017). Review on effect of various types of reinforcement particles on mechanical behavior of 6061 and 7075 aluminium alloy matrix composites. International Journal of Emerging Technologies in Engineering Research. 5(8), 100 – 104.

Wang, X.; S. Liu and Y. Lin. (2022). Effect of Zn and Cu addition on microstructure and mechanical properties of Al-10wt%Mg alloy. Metals. 12, 1027. https://doi.org/10.3390/met12061037.

Wu, X. F.; Z. C. Wang; T. Cheng; K. Wang; J. Xiang; R. Zhao; S. H. Chen and F. Wu (2022). Effects of Cu addition on microstructure and mechanical properties of Er-modified Al-$10Mg_2Si$ cast alloys. Journal of Central South University. 29, 795 – 806. https://doi.org/10.1007/s11771-022-4963-3.

Zawrah M. F.; W. M. El-Meligy; H. H. A. Saudi; S. Ramadan and M. A. Taha (2022). Mechanical and electrical properties of nano Al-matrix composites reinforced with SiC and prepared by powder metallurgy. Biointerface Research in Applied Chemistry. 12(2), 2068 – 2083. https://doi.org/10.33263/BRIAC122.20682083.